Impact of the end of range damage from low energy Ge preamorphizing implants on the thermal stability of shallow boron profiles

R. A. Camillo-Castillo
SWAMP Center, Department of Materials Science and Engineering, University of Florida, Gainesville, Florida 32611

M. E. Law
SWAMP Center, Department of Electrical and Computer Engineering, University of Florida, Gainesville, Florida 32611

K. S. Jones
SWAMP Center, Department of Materials Science and Engineering, University of Florida, Gainesville, Florida 32611

(Received 8 March 2004; accepted 7 June 2004)

A fundamental understanding of the effect of scaling amorphous layers on the thermal stability of active concentrations is required for the formation of ultrashallow junctions. A study on the influence of boron on the evolution of the end of range defects for samples containing shallow amorphous layers formed by low energy germanium implants is conducted. Czochralski grown (100) silicon wafers are preamorphized with 1×10^{15} cm^{-2}, 10 keV Ge^+ and subsequently implanted with 1×10^{15} cm^{-2}, 1 keV B^+ such that high boron levels are attained in the end of range region. A sequence of anneals are performed at 750 °C, under nitrogen ambient for times ranging from 1 s to 6 h and the end of range defect evolution is imaged via plan-view transmission electron microscopy (TEM). Defect analyses are conducted utilizing quantitative TEM which indicates substantial differences in the defect evolution for samples with boron in the end of range. The extended defects observed are very unstable and undergo a fast dissolution. In contrast, stable defects are observed in the experimental control in which the evolution follows an Ostwald ripening behavior. Secondary ion mass spectroscopy analyses confirm the ephemeral nature of the defects observed and also demonstrates drastic reductions in interstitial supersaturation. In addition, uphill-type diffusion is observed to occur for a short time frame, which emphasizes a transient interstitial supersaturation. Correlation of this data with sheet resistance and active dose measurements conducted on a Hall measurement system strongly indicates the formation of boron interstitial clusters. The high boron concentrations and supersaturation levels attained at the anneal temperature enables the cluster formation. An estimate of the boron concentrations trapped in the clusters is determined from the active dose obtained from the Hall measurements and indicates concentrations much higher than those available in the end of range. This suggests an interstitial migration from the end of range to regions of higher boron levels. Since the end of range is in the vicinity of the highly doped layer it is not isolated from the strain effects induced by the high initial activation levels. Hence it is proposed that the tensile strain stimulates the interstitial migration from the end of range to the boron-doped layer. Consequently, the end of range defects dissolve as the interstitial supersaturation falls below levels required to sustain their evolution. © *2004 American Institute of Physics*. [DOI: 10.1063/1.1776624]

INTRODUCTION

Standard complementary metal-oxide semiconductor technology currently employs the formation of amorphous layers via ion implantation prior to the introduction of the dopant atoms into the silicon lattice, to reduce channeling effects, thus allowing the formation of shallow, doped layers. Although the ion implantation technique offers a number of advantages, this nonequilibrium process results in an inherent damage to the crystal lattice. Annealing following the implantation repairs the lattice damage and activates the implanted dopant atoms. The high interstitial supersaturation in the silicon lattice during the annealing process allows for a number of complex and coupled processes such as clustering, diffusion and dopant deactivation. The thermal budget to which the material is subjected results in thermal diffusion of the implanted dopants and therefore increased junction depths. A transient enhanced diffusion[1] (TED) also occurs due to the formation of mobile dopant complexes via the coupling of silicon interstitials with the substitutional dopant atoms, resulting in even deeper junctions. A substantial amount of research has been devoted to understanding the nature of the TED and its relation to the end of range (EOR) damage[2–5] that accompanies amorphization. It is widely accepted that the point defects generated by the amorphization process agglomerate to form submicroscopic interstitial clusters, which are precursors for the nucleation of 311-type defects. The unfaulting of the 311-type defects result in the formation of dislocation loops. These EOR defects act as

both a source and sink for excess silicon interstitials and therefore provide the necessary interstitial supersaturation for TED.

Solid phase epitaxial regrowth is capable of activating dopant levels that exceed solid solubility levels in silicon, at relatively low temperatures. The low thermal budget applied to the lattice offers many advantages including minimal diffusion and therefore good junction depth control. This is highly beneficial for achieving the ultrashallow junctions that the International Technology Roadmap for Semiconductors[6] demands. In addition, it provides excellent compatibility with the thermal requirements of high-K dielectric materials and metal gates. As the industry attempts to achieve highly doped, shallow layers, ultra low energy (ULE) dopant ion implantation is becoming increasingly important. These ULE implants do not require deep amorphous layers to eliminate channeling and therefore, lower energy preamorphizing implants can be used. Low energy amorphizing implants have the advantage of producing a reduced number of recoil atoms into the EOR. Thus, there are fewer interstitial atoms in the structure that can contribute to TED. However, lowering the implant energy reduces the distance from the EOR region to the surface and also results in high interstitial supersaturations in the vicinity of the dopant profile. As the dominant p-type dopant in silicon, boron has been studied extensively. The high interstitial concentrations generated by the ion implantation process have been demonstrated to result in the clustering of boron atoms at concentrations far below its solid solubility.[7] The resultant boron interstitial clusters drastically deteriorate the electrical properties of the material. The proximity of the EOR formed by the amorphizing implant to the boron profile therefore raises many concerns and questions regarding the thermal stability of the activated junctions and the effect that the boron presence has on the EOR defect evolution.

EXPERIMENT

Czochralski grown, 200 mm, n-type Si wafers of (100) orientation were preamorphized with 10 keV, 1×10^{15} cm^{-2} Ge^+ ions at a tilt and twist of 5° and 0°, respectively, producing a 23 nm continuous amorphous layer extending from the surface. B^+ ions were then implanted at an energy of 1 keV and a dose of 1×10^{15} cm^{-2}, under similar implant conditions. Wafers without a subsequent B^+ implant served as the experimental control. Both sets of wafers were cut into 1.4×1.4 cm^2 samples and simultaneously annealed under a nitrogen ambient at 750 °C for times ranging from 1 to 6 h. Anneals performed for less than 5 min were conducted in an Abrikosov-Gorkov Associates Heat Pulse 210 T Rapid Thermal Annealer (RTA). The RTA temperature profile consisted of a 600 °C, 10 s soak and a ramp to 750 °C at a rate of 100 °C s^{-1}. Furnace anneals were utilized for anneal times exceeding 5 min and were executed in a quartz tube furnace.

Subsequent to annealing a series of analytical techniques were employed to examine the silicon lattice. The microstructure was analyzed for extended defects via plan-view transmission electron microscopy (PTEM) performed on a JOEL 200 CX, operating at an accelerating voltage of 200 keV. PTEM samples were prepared by standard HF/HNO_3 backside etching methods and were imaged at g_{220} weak beam dark field (WBDF) conditions. The quantification technique of Bharatan *et al.*[8] was employed in the defect density analysis. Cross-sectional TEM sample preparation entailed ion milling with a 5 kV Ar^+ beam produced from plasma sources tilted at 12° to the surface plane. These images were taken under g_{110} bright field diffraction conditions and were used to confirm amorphous layer depths measured by variable angle spectroscopic ellipsometry (VASE). The VASE measurements were performed on a J.A. Woollam EC110 multiwavelength ellipsometer with the 75 W Xe light source at 25° to the surface. The measurements were conducted at 65 °, 70° and 75°. Dopant concentration-depth profiles were assessed by secondary ion mass spectroscopy (SIMS) using an Adept 1010 Dynamic SIMS System by Physical Electronics. A 50 nA, 2 kV oxygen beam was employed at 41° to the normal to the surface with a raster of $250\otimes250$ mkm^2. Sheet resistances were measured on a MMR Technologies Inc., Hall and Van der Pauw Measurement System. These measurements were conducted at 90 K to reduce errors associated with leaky junctions, which result in contributions from the n-type substrate,[9] thus allowing reliable sheet resistance measurements.

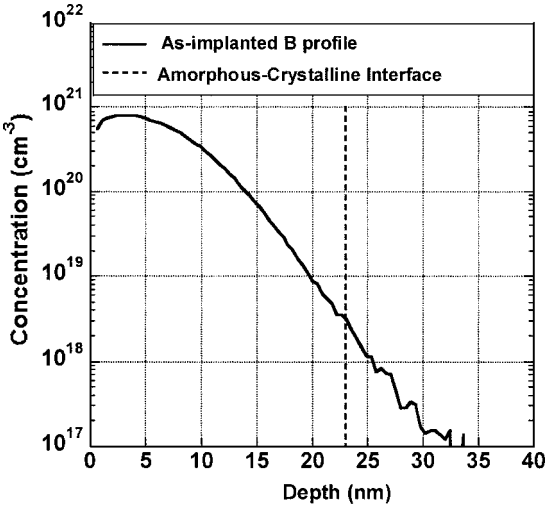

FIG. 1. As-implanted boron concentration-depth profile for sample containing a 1 keV, 1×10^{15} cm^{-2} B^+ and 10 keV, 1×10^{15} cm^{-2} Ge^+ implants, indicating the amorphous-crystalline interface.

RESULTS AND DISCUSSION

The B^+ implant conditions were chosen such that the boron is positioned in the vicinity of the end of range and is not wholly confined to the amorphous region. Figure 1 is the boron concentration-depth profile for the as-implanted case, obtained from SIMS analysis. The boron implant produced a peak concentration of $\sim9\times10^{20}$ cm^{-3} and a junction depth of 26 nm, measured at a concentration of 1×10^{18} cm^{-3}. It is evident at the amorphous-crystalline interface the boron concentration is on the order of 3×10^{18} cm^{-3} and extends into the EOR region. In an attempt to explore the evolution of the EOR defects for 10 keV Ge^+ preamorphization, an anneal temperature of 750 °C was selected, based on the findings of

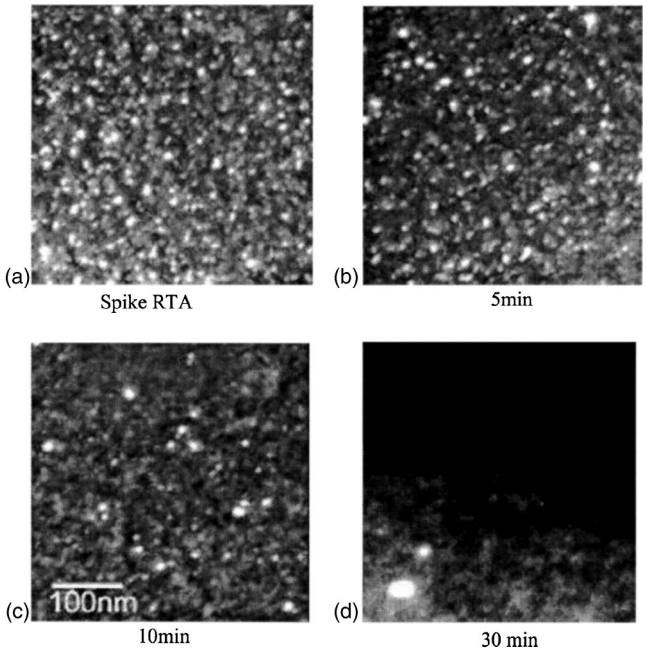

FIG. 2. PTEM WBDF images taken at g_{220} imaging conditions of the extended defects for samples containing 1 keV, 1×10^{15} cm^{-2}B^{+} and 10 keV, 1×10^{15} cm^{-2}Ge^{+} implants. Annealed at 750 °C.

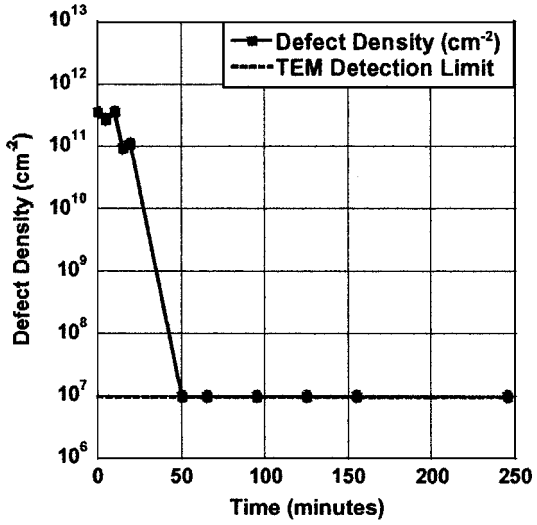

FIG. 3. Defect density as a function of annealing time for samples containing 1 keV, 1×10^{15} cm^{-2} B^{+} and 10 keV, 1×10^{15} cm^{-2} Ge^{+} implants. Annealed at 750 °C.

Gutierrez.[10] His findings indicate stable, dislocation loops are the prime defect structure for a similar Ge^{+} amorphizing implant annealed at 750 °C. In addition, the defect evolution follows an Ostwald ripening behavior in which large defects grow at the expense of the smaller ones by the interchange of atoms. This is exhibited by an increase in defect size and simultaneous decrease in the defect density.

PTEM images of the defect evolution at 750 °C for samples containing Ge^{+} and B^{+} implants are shown in Fig. 2. Dotlike, interstitial clusters populate the microstructure and are visible for annealing times of up to 10 min. The defect structure seems to undergo few changes, as the defect morphology appears very similar. But, it is clear that the number of defects in the lattice has decreased in a very short annealing time. This trend becomes clearer on investigating the microstructure after 30 min of annealing, since most of the interstitial clusters have dissolved. Figure 3 depicts the defect density as a function of annealing time in which the rapidity of the defect dissolution is more pronounced. It is evident that the density is on the order of 3.5×10^{11} cm^{-2} after a spike anneal at 750 °C and decreases to $\sim1\times10^{11}$ cm^{-2} after 20 min of annealing. But the density undergoes a drastic reduction to values below the detection limit of the TEM, after a 30 min anneal. Examination of the microstructure of the experimental control, which contains no subsequent B^{+} implant, indicates a substantial difference in the defects observed and their evolution. The extended defects are illustrated in Fig. 4 via PTEM images. The microstructure in the initial stages of annealing appears very similar to that of samples containing boron. Nevertheless, distinct differences can be discerned as early as 10 min into the annealing process. It is evident that the interstitial clusters have begun to coalesce into more stable configurations, such as 311-type defects. Sustained annealing results in the formation of stable dislocation loops, which are seen to coarsen and eventually dissolve. The defect evolution unambiguously follows an Ostwald ripening process. Figure 5 is a

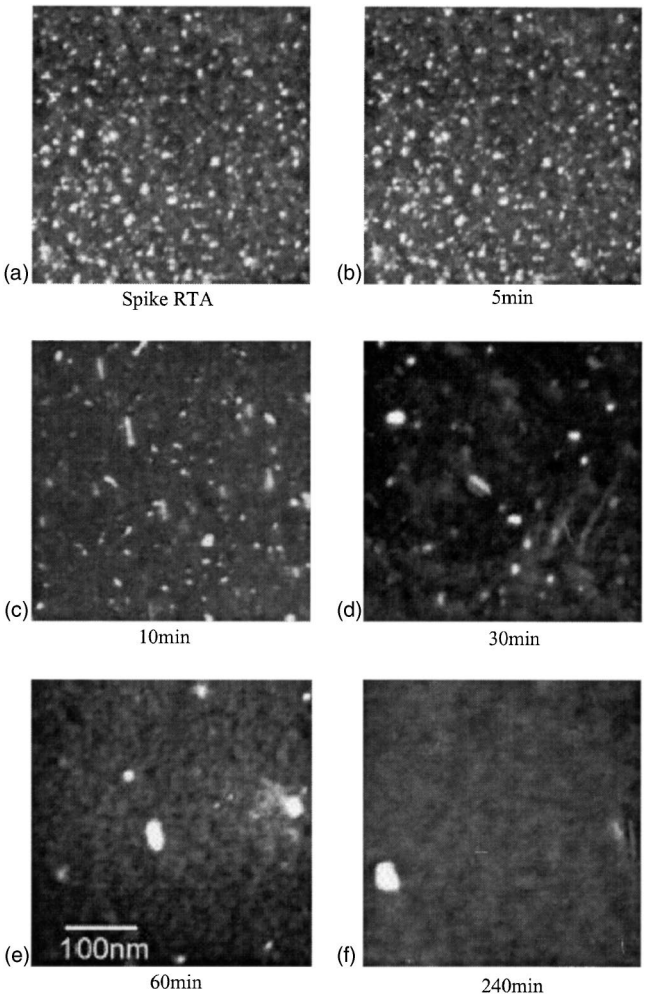

FIG. 4. PTEM WBDF images taken at g_{220} imaging conditions of the extended defects for samples containing 10 keV, 1×10^{15} cm^{-2} Ge^{+} implants. Annealed at 750 °C.

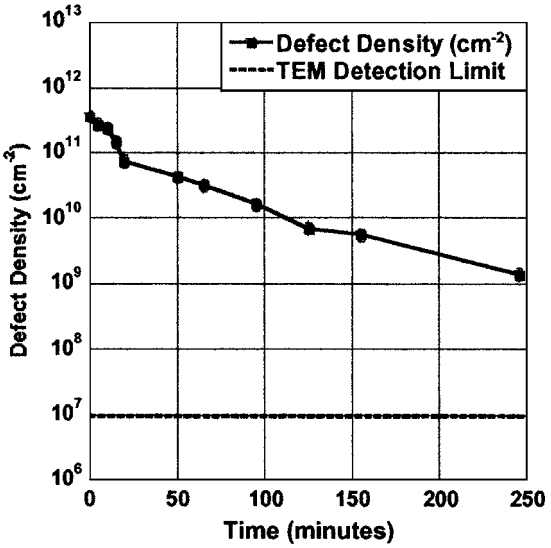

FIG. 5. Defect density as a function of annealing time for samples containing 10 keV, 1×10^{15} cm^{-2} Ge^+ implants. Annealed at 750 °C.

plot of the defect density versus annealing time. The defect densities attained in the initial stages of the anneal are comparable to those observed for samples containing a B^+ implant and are on the order of 3.5×10^{11} cm^{-2}. However, beyond 30 min a rapid dissolution is not observed, rather the defect evolution appears to follow an exponential decay. These considerable differences in the defect evolutions indicate that the B^+ presence has some influence on the defect behavior.

To gain a better understanding of the role boron plays in the defect evolution, SIMS analysis was conducted to track the boron diffusion with time. Figure 6 depicts the boron concentration-depth profiles for anneal times up to 30 min. One of the most conspicuous features of the profile is the evolving boron pileup at ~27 nm, in the vicinity of the EOR. This diffusion behavior is consistent with previous reports of boron gettering to the EOR.[11] After 5 min of annealing the initial stages of gettering are noticeable by the presence of a shoulder in the concentration profile, which develops into a distinct peak at a concentration of 7×10^{18} cm^{-2}, after 10 min. Conversely, no boron pile up at the EOR region is evident after 30 min of annealing, suggesting dissolution of the damage. This outcome concurs with the observations of the PTEM analysis, which verified few EOR defects after 30 min of annealing. In addition, a TED occurs between 5 and 10 min resulting in an increase in the junction depth of ~15 nm. It is well established that TED is due to the formation of mobile complexes via the coupling of boron atoms with the excess silicon interstitials.[1] This observed diffusion is therefore indicative of a high ephemeral interstitial supersaturation into the bulk silicon. Beyond this time the diffusion observed is considerably less and it can be deduced that the interstitial supersaturation has diminished.

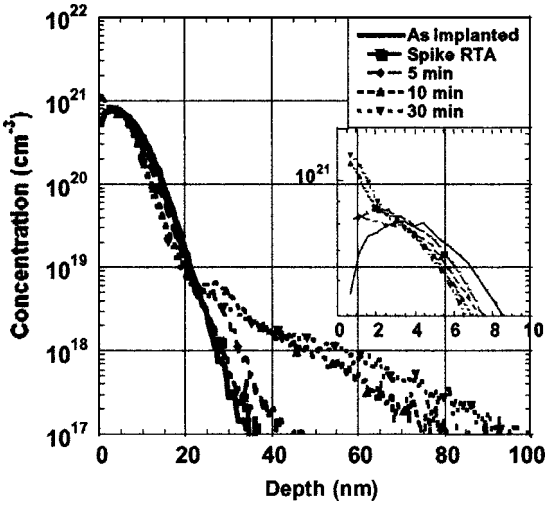

FIG. 6. Boron concentration-depth profiles for samples containing a 1 keV, 1×10^{15} cm^{-2} B^+ and 10 keV, 1×10^{15} cm^{-2} Ge^+ implants. Annealed at 750 °C.

Further examination of these profiles, reveals diffusion characteristics that are consistent with previous reports of boron uphill diffusion.[12,13] Similar to reports by Duffy *et al.*,[12] boron concentrations exceeding 5×10^{18} cm^{-3} have moved towards the surface. This motion is evident for all of the concentration profiles and progresses from 1 nm to 1.9 nm between the spike and 30 min anneals, respectively. The boron dose for each profile was extracted from the SIMS analysis and indicates boron dose loss occurs during the anneal. This can account for the shift in the profiles toward the surface. In addition to this shift, the profiles obtained after 10 and 30 min of annealing indicate boron concentrations at the surface on the order of 1×10^{21} cm^{-3}, which exceed the as-implanted surface concentration and may be indicative of an uphill diffusion. Recently, Cowern *et al.*[14] suggested that the steep gradients in interstitial supersaturation to the surface provide efficient boron transport to the Si/SiO_2 interface. Careful inspection of the profiles indicates a large increase in the surface concentration occurs between 5 and 10 min. This relatively large increase in the boron surface levels implies a high interstitial flux to the surface that may be driven by a large gradient in the interstitial supersaturation between the defect layer and the surface. As annealing advances to 30 min, however, the surface boron concentration undergoes a small increase. This is an indication of a decline in the surface interstitial flux and hence a reduction in the driving force for interstitial diffusion. These observations, together with the lower diffusion levels observed between 10 and 30 min in the tail of the profiles, clearly illustrate the interstitial supersaturation in the lattice falls. However, this time interval also coincides with the rapid release of trapped interstitials from the EOR defects, which does not correlate with the corresponding uphill and tail diffusion observed and suggests the existence of another sink for the released interstitials.

In order for interstitial clusters to follow an Ostwald ripening behavior and evolve into more stable structures, a certain interstitial supersaturation is required. If the supersaturation falls below this level, the defects dissolve releasing the trapped interstitials in an attempt to sustain the high interstitial levels in their vicinity. Consequently, further evolution cannot occur. These results indicate that for samples containing boron, defect dissolution occurs rapidly, which is symp-

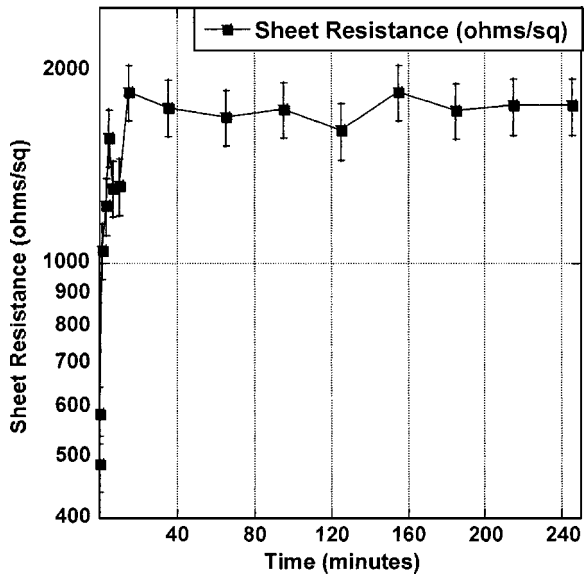

FIG. 7. Sheet resistance vs anneal time for samples containing a 1 keV, 1×10^{15} cm^{-2} B^+ and 10 keV, 1×10^{15} cm^{-2} Ge^+ implants. Annealed at 750 °C.

tomatic of a drastic decrease in the interstitial supersaturation. The SIMS analyses also point toward lower levels of interstitial supersaturation. On the other hand, in samples without boron, the EOR defects are seen to evolve into stable, dislocation loops indicating that the interstitial supersaturation is not depleted. It is therefore reasonable to infer that the boron presence influences the interstitial supersaturation in the vicinity of the EOR defects. This may be due to boron clustering with the interstitial atoms. It is well established that boron interstitial clustering occurs when a highly doped region is subjected to an interstitial supersaturation.[7] The boron implant conditions employed in this experiment confines the boron atoms to the vicinity of the surface resulting in high surface levels of $\sim1\times10^{21}$ cm^{-3}. Furthermore, high concentrations are also attained in the EOR region. At 750 °C, the interstitial supersaturation should be on the order of 1×10^4 according to the findings of Cowern *et al.*[15] Therefore, the necessary conditions exist to enable clustering effects and BIC formation. BICs grow by binding interstitials until a high supersaturation is sustained.[16,17] It is therefore postulated that the BICs compete with the EOR defects for the interstitial supersaturation.[18,19] Consequently, the interstitial supersaturation in the defect band falls during the boron clustering process and is eventually not high enough to support the defect existence and evolution.[20]

Understanding the electrical behavior of boron is key to gaining further insight into the processes governing the defect evolution. BICs are known to severely deteriorate the electrical properties of the silicon host due to boron electrical deactivation[21,18] and carrier concentration mobility lowering.[22] They have also been shown to be very stable, existing for up to 4 h after TED at 800 °C.[7,22] Boron activation data, measured by Hall effect, show rapid boron deactivation (Figure 7). A spike anneal at 750 °C achieves a minimum sheet resistance of 489 Ω/□. Further annealing at this temperature, however, results in a rapid deactivation. There is an abrupt increase in sheet resistance, within a 15 min period to value of 1750 Ω/□, at which point it saturates. Measurements conducted on samples annealed up to 4 h demonstrate no improvements in the boron activation, suggesting that the boron exists in a stable configuration. These deactivation characteristics are consistent with the formation of BICs. The fact that the deactivation process saturates implies that the supersaturation may have fallen to levels that are too low to support further BIC formation. The time at which this occurs is consistent with the fall in supersaturation observed in the SIMS data and the rapid defect dissolution process associated with the lower interstitial levels.

BIC formation is typically associated with an immobile peak concentration. The SIMS results presented here, however, do not exhibit this characteristic; rather the profiles display an uphill diffusion motion. This may be explained by the fact that the immobile portion of the profile is hidden. An estimate of the clustered concentrations can be obtained from the inactive portion of the dose, which is determined from the Hall measurements. The total dose used is extracted for each profile from the SIMS analysis. The calculated clustered concentrations are $\sim1\times10^{20}$ cm^{-3} and are below the maximum boron concentration, which would explain why the immobile portion of the profiles is not evident. In addition, these inactive boron concentrations are two orders of magnitude higher than the boron concentrations located in the EOR, which suggests that boron deactivation is not confined to the EOR region. There are also no indications of clustering in the EOR in the SIMS data, as the profiles are seen to move. Deactivation of boron atoms in the regrown crystal by clustering necessitates the migration of interstitial atoms from the EOR to regions of high boron concentration. However, the driving force for this motion is unclear. It is evident in the experimental control that interstitial annihilation at the surface does not play a role in the defect evolution.[23] It is therefore reasonable to assume the surface does not play a role in the reduced interstitial supersaturations and thus, in the interstitial migration from the EOR. One possible explanation for such motion is that the silicon interstitials diffuse to the regions of higher boron concentration to compensate the strain fields associated with the initial high concentration of substitutional boron atoms. This migration is plausible since the EOR region is in close proximity to the strained substitutional boron region and therefore may not be isolated from the effects of the strained layer. The tensile strain hence is the stimulus for interstitial migration. The interstitials interact with the substitutional boron atoms to form BICs, which then continue to bind the interstitials competing with the EOR for the interstitial supersaturation. Hence the EOR defects never evolve into more stable structures.

CONCLUSION

The boron presence in the vicinity of the EOR plays a fundamental role in the EOR defect evolution. The rapid dissolution of the EOR damage in samples containing boron signifies a decrease in the interstitial supersaturation. In addition, the rapidity of the observed junction deactivation is

consistent with the formation of boron interstitial clusters. This strongly suggests that the BIC formation is responsible for the drastic reduction in interstitial supersaturation in the defect band, which is required for the formation of stable defects. The tensile strain associated with the initial high boron activation may induce interstitial migration from the EOR to the strained layer resulting in BIC formation and the corresponding deactivation observed. Consequently, the supersaturation in the EOR falls to levels that are too low to sustain the defect evolution and ultimately they dissolve.

The thermal stability of the junction is strongly influenced by the proximity of the interstitial concentrations associated with the EOR. These findings suggest that highly doped layers need to be isolated from the effects of the supersaturation in the EOR, which necessitates the formation of deeper amorphous layers.

[1]A. E. Michel, W. Rausch, P. A. Ronsheim, and R. K. Keitl, Appl. Phys. Lett. **50**, 417 (1987).
[2]L. H. Zhang, K. S. Jones, P. H. Chi, and D. S. Simons, Appl. Phys. Lett. **67**, 2025 (1995).
[3]H. G. A. Huizing, C. C. G. Visser, N. E. B. Cowern, P. A. Stolk, and R. C. M. de Kruif, Appl. Phys. Lett. **69**, 1211 (1996).
[4]J. L. Benton, S. Libertino, P. Kringhoj, D. J. Eaglesham, and J. M. Poate, J. Appl. Phys. **82**, 120 (1997).
[5]S. Coffa, S. Libertino, and C. Spinella, Appl. Phys. Lett. **76**, 321 (2000).
[6]International Technology Roadmap for Semiconductors, http://public.itrs.net/Files/2003ITRS/Home2003.htm
[7]P. A. Stolk, H-J. Gossmann, D. J. Eaglesham, D. C. Jacobson, J. M. Poate, and H. S. Luftman, Appl. Phys. Lett. **66**, 568 (1994).
[8]S. Bharatan, J. Desrouches, and K. S. Jones, *Materials and Process Characterization of Ion Implantation* (Ion Beam, 1997) Vol. 4, p. 222.
[9]S. H. Jain, P. B. Griffin, and J. D. Plummer, J. Appl. Phys. **93**, 1060 (2003).
[10]A. F. Gutierrez., Master's thesis, University of Florida, 2001.
[11]C. Bonafos, A. Claverie,D. Alquier, C. Bergaud, A. Martinez, L. Laanab, and D. Mathiot, Appl. Phys. Lett. **71**, 365 (1997).
[12]R. Duffy, V. C. Venezia, H. Heringa, T. W. T. Husken, M. J. P. Hopstaken, N. E. B. Cowern, P. B. Griffin, and C. C. Wang, Appl. Phys. Lett. **82**, 3647 (2003).
[13]H. C. Wang, C. C. Wang, C. S. Chang, T. Wang, P. B. Griffin, and C. Diaz, IEEE Electron Device Lett. **22** (2001).
[14]N. E. B. Cowen *et al.*, Mater. Res. Soc. Symp. Proc. **765**, D.6.8.1 (2003).
[15]N. E. B. Cowern, G. Mannino, P. A. Stolk, F. Roozeboom, H. G. A. Huizing, J. G. M. van Berkum, F. Cristiano, andA. Claverie, Phys. Rev. Lett. **82**, 4460 (1999).
[16]L. Pelaz, G. H. Gilmer, H-J. Gossmann, C. S. Rafferty, M. Jaraız, andJ. Barbolla, Appl. Phys. Lett. **74**, 3657 (1999).
[17]G. Mannino, N. E. B. Cowern, F. Roozeboom, and J. G. M. van Berkum, Appl. Phys. Lett. **76**, 855 (2000).
[18]A. D. Lilak, S. K. Earles, M. E. Law, and K. S. Jones, Appl. Phys. Lett. **74**, 2038 (1999).
[19]T. E. Haynes, D. J. Eaglesham, P. A. Stolk, H-J. Gossman, D. C. Jacobson, and J. M. Poate, Appl. Phys. Lett. **69**, 1376 (1996).
[20]G. Mannino, V. Privitera, S. Solmi, N. E. B. Cowern, Nucl. Instrum. Methods Phys. Res. B **186**, 246 (2002).
[21]N. E. B. Cowern, K. T. F. Janssen, and H. F. F. Jos, J. Appl. Phys. **68**, 6191 (1990).
[22]S. Mirabella, E. Bruno, F. Priolo, D. De Salvador, E. Napolitani, A. V. Drigo, and A. Carnera, Appl. Phys. Lett. **83**, 680 (2003).
[23]A. C. King, A. F. Gutierrez, A. F. Saavedra, K. S. Jones, and D. Downey, J. Appl. Phys. **93**, 2449 (2003).